

## Research Article

# Research on Optimization of Large Flow Hydraulic Punching Process in Zhaozhuang Mine

Jiabao Zhang and Dingqi Li 

*School of Energy Science and Engineering, Henan Polytechnic University, Jiaozuo 454003, China*

Correspondence should be addressed to Dingqi Li; [ldingqi1979@163.com](mailto:ldingqi1979@163.com)

Received 8 June 2022; Revised 20 September 2022; Accepted 28 September 2022; Published 29 December 2022

Academic Editor: Qingquan Liu

Copyright © 2022 Jiabao Zhang and Dingqi Li. This is an open access article distributed under the Creative Commons Attribution License, which permits unrestricted use, distribution, and reproduction in any medium, provided the original work is properly cited.

Taking hydraulic punching test of Zhaozhuang Mine as engineering background, by comparing the field application effects of different hydraulic punching processes, the relationship between coal moisture content around the borehole blockage and gas extraction effect was monitored and analyzed. The following conclusions were drawn: the occurrence of borehole blockage was the result of the comprehensive action of coal slag particle size and slag discharge capacity of punching return water. Blocking the borehole led to the accumulation of a large amount of punching high-pressure water and coal slag in the borehole, which compressed and infiltrated the surrounding coal body and reduced gas extraction efficiency of borehole. Under the condition of the same amount of coal produced by punching, the different punching methods led to the great difference in the influence radius of punching. The large flow three-stage coal-breaking hydraulic punching system developed according to the borehole blockage mechanism can effectively reduce the particle size of coal slag, increase the punching flow, effectively avoid borehole blockage, and improve gas extraction efficiency of borehole.

## 1. Introduction

With the continuous development of the world economy, human society's demand for energy is growing, what is more, environmental protection and energy issues are becoming more and more prominent [1]. Methane is a kind of high-calorific value clean energy source [2] and is the second largest greenhouse gas [3, 4]. As the world's largest producer and consumer of coal [5], China accounts for 90% of the total emissions from the entire national energy sector in coal mining alone [6], and such a large amount of gas is directly emitted into the atmosphere, causing serious environmental pollution problems [7, 8]. Therefore, improving the efficiency of gas extraction and avoiding gas discharge into the air is the key to solving the problem of converting gas from a harmful gas to a clean energy source [2, 9, 10]. By decompressing the coal seam, the permeability of the seam can be effectively improved, and the efficiency of gas extraction can be enhanced. Liquid nitrogen fracturing [11], microwave fracturing [12], and CO<sub>2</sub> blasting fracturing [13] are effective in decompressing the

coal seam, but the cost is high, which restricts the application. Deep borehole blasting [14] is more dangerous. Hydraulic measures are technically mature, moderate in cost, widely used, and have significant pressure relief effects. However, hydraulic fracturing [15] with water injection pressure up to 100 MPa requires high equipment performance and operator requirements. Hydraulic slitting [16] has coal joints that are prone to collapse, which affects the scope of pressure relief. Hydraulic punching [17] requires relatively moderate water pressure, is less technically difficult, and is the most widely used in hydraulic gas management technology.

However, the current research on hydraulic punching technology concentrates upon the influence of punching on the efficiency of gas extraction [18], the relationship between the coal output and the pressure relief range [19], the research on the safe water pressure for punching [20], and the research on the mechanism of water jet damage to coal seams [21]. The lack of in-depth research on solving the phenomenon of blockage and spraying boreholes in the process of punching, as well as the problem of difficult

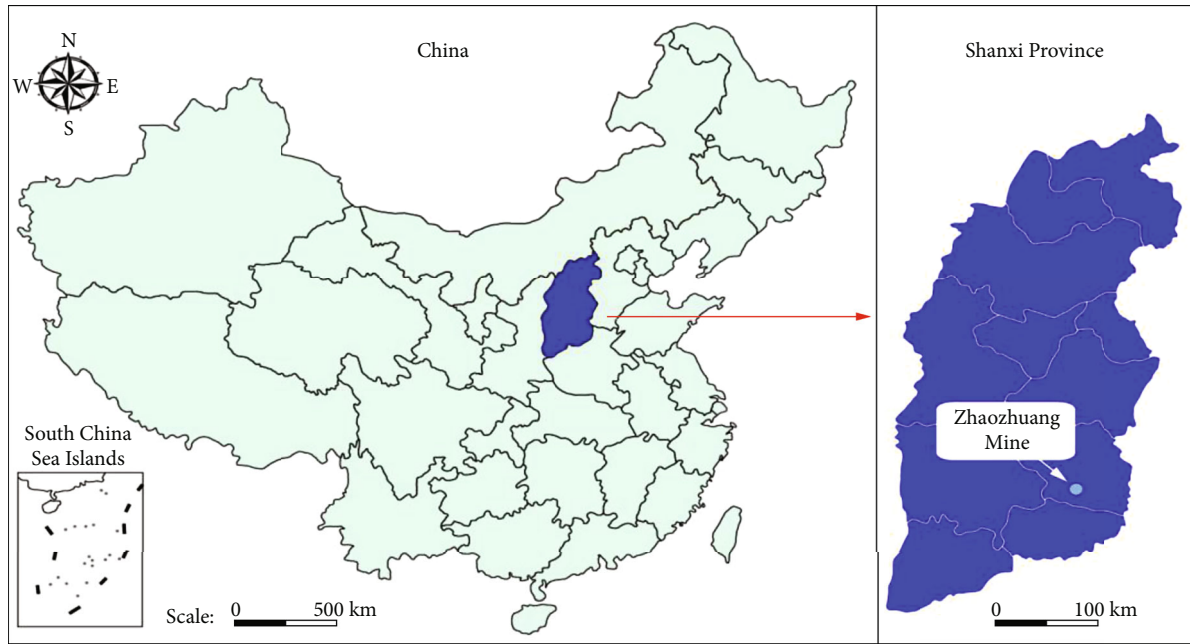


FIGURE 1: Location of Zhaozhuang Mine.

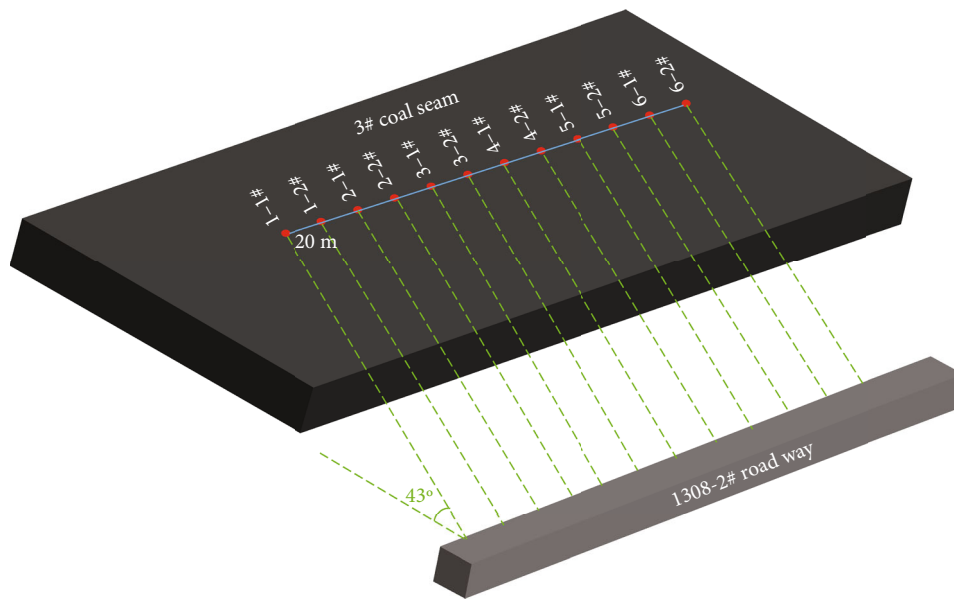


FIGURE 2: Layout of boreholes in the first test area.

control of coal output, has restricted the promotion of hydraulic punching technology. The author proposed a large flow three-stage coal breaking hydraulic punching process based on a comprehensive consideration of the influence of various factors on the punching effect through a field test of hydraulic punching in Zhaozhuang Mine and verified the feasibility and superiority of the punching process on site.

## 2. Hydraulic Punching Test Scheme and Device

**2.1. Test Site and Punching Scheme.** As shown in Figure 1, Zhaozhuang Mine is part of Jincheng Coal Group in Shanxi

Province, China, and it is located in the southeast of the Qinshui coalfield. The mine is situated in 53 km north of Jincheng, 12 km north of Gaoping City, and 16 km south of Zhangzi County. The designed annual productive capacity of Zhaozhuang Mine is 8 million tons. The area of mine field is 144.1 km<sup>2</sup>, and the minable coal is located in seams of No.3 and No.15. At present, only the top coal seam (No.3) can be exploited. From an evaluation of gas from coal seam No. 3, the relative gas gushing quantity under the mine was found to be 9.82 m<sup>3</sup>/t, and the absolute gas gushing quantity was 98.94 m<sup>3</sup>/min. Therefore, the Zhaozhuang Mine is considered a high-gas mine [22].

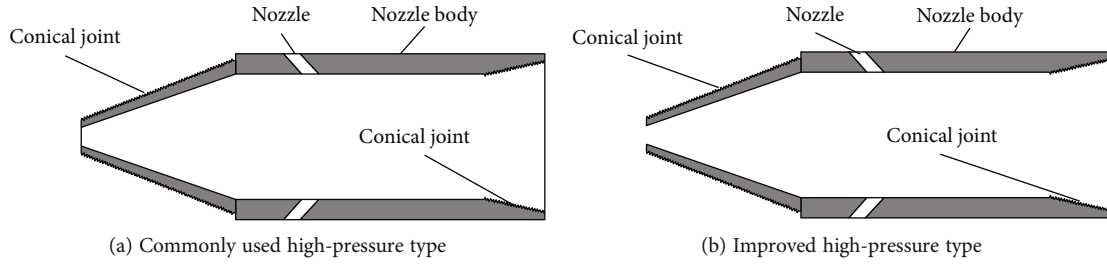


FIGURE 3: High-pressure type used in punching tests.

In Zhaozhuang Mine, the test site was arranged in the eastern section of the floor roadway of No. 1308-2. The net width and height of the roadway were 5 m and 3 m, respectively. The distance between No. 1308-2 floor rock roadway and No. 3 coal seam was 7 m. In the north wall of the roadway, sets of boreholes were arranged every 20 m. In each sets, two boreholes were designed, the horizontal spacing between the boreholes of No. 1 and No. 2 was 20 m. The hydraulic punching test was only carried out for borehole of No. 1. The normal borehole of No.2 acted as a reference to compare the gas extraction effect of the punched borehole. The diameters and pattern inclinations of both No.1 and No.2 boreholes were 165 mm and  $43^\circ$ , respectively, and each borehole extended 6 m into the coal seam. There were 18 sets altogether in this test according to the location of boreholes, which were divided into three punching regions. As the layouts of boreholes in each punching region were the same, only the layout of boreholes in the first punching region is presented, as shown in Figure 2. Because the ventilation quantity in the roadway was relatively small, it was necessary to prevent the gas concentration from exceeding the safety limit during punching based on safety consideration.

**2.2. Hydraulic Punching Device System.** The hydraulic punching system was mainly composed of the following equipment: drilling rig for punching, high-pressure water pump, high-pressure round drill rod, high-pressure triangular drill pipe, high-pressure nozzle, and a high-pressure water hose.

**2.2.1. Drilling Rig for Punching.** The drilling rig adopts ZDY series mobile drill that can move by crawler walking and accepted all types of punched drill pipe with a diameter of 73 mm. The drilling tool could be screwed and removed mechanically and automatically, thus alleviating the demand on workers and improving the work efficiency.

**2.2.2. High Pressure Nozzle.** As shown in Figure 3, the high-pressure nozzle is the key equipment for achieving high-pressure coal breaking during hydraulic punching. During the tests, a commonly used high-pressure nozzle and the improved high pressure nozzle were adopted alternately. They both resisted high pressure of 40 MPa. In Figure 3(a), three high-pressure nozzles with an orifice diameter of 3 mm were distributed uniformly radially around the barrel. The improved high-pressure nozzle

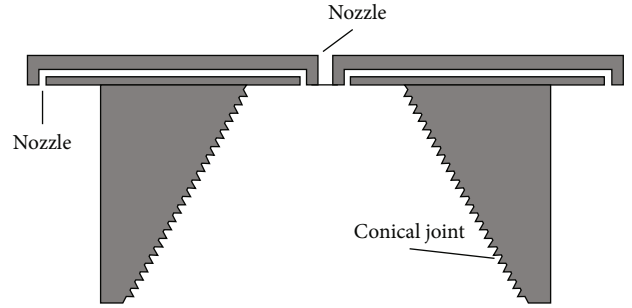


FIGURE 4: Flow-increasing and cinder-breaking device for conveying cinder.

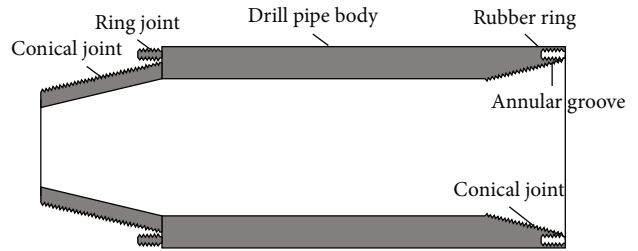


FIGURE 5: Improved high-pressure drill pipe.

TABLE 1: Test parameters in the first punching area.

Borehole number	Quality of discharge (t)	Jet pressure (MPa)	Jet flow (L/min)
1-1#	4	15	208
2-1#	4.6	16	215
3-1#	3	16	215
4-1#	5	17	221
5-1#	3.5	15	208
6-1#	6	17	221

featured an opening at the front of high-pressure nozzle barrel head that connected to a flow-increasing device for conveying broken cinder; in addition, the recrushing and flow back capability were reinforced. In Figure 3(b), the conical joint was used to connect the drill pipe to the broken cinder flow-increasing device.

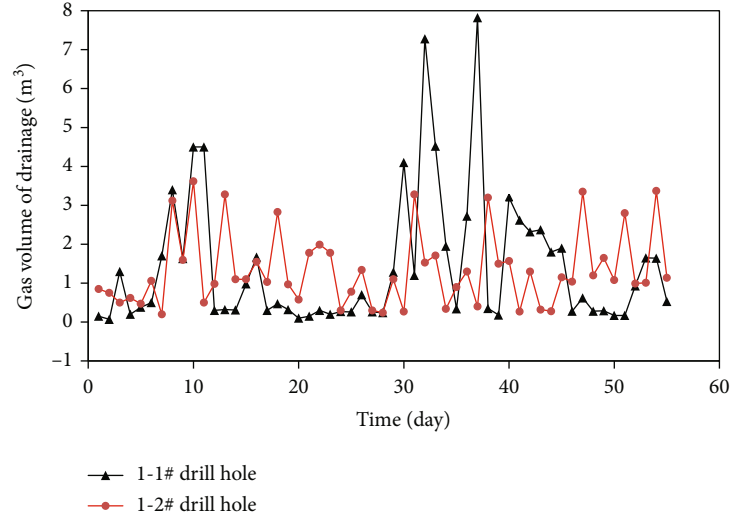


FIGURE 6: Gas extraction in the borehole group 1#.

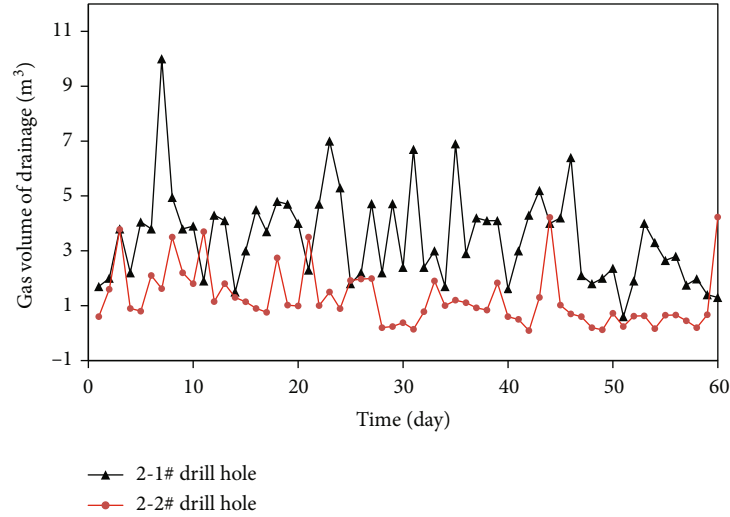


FIGURE 7: Gas extraction in the borehole group 2#.

**2.2.3. Flow-Increasing Device for Broken Cinder.** As shown in Figure 4, the flow-increasing device to convey broken cinder consisted of three nozzles 2 mm each diameter. In the center of the device, a forward nozzle was provided to impact and break the coal during borehole collapse and drill pipe pressing. When there was no borehole collapse and drill pipe pressing, the backflow high-pressure water served to increase the deslagging flow. The other two backward-facing nozzles were arranged opposite each other at the outer edge of the device. The backward nozzles were oriented parallel to the central axis of the device, and the spray force from the nozzles offset the forward spray force of the high-pressure nozzle, helping to propel the high-pressure nozzle during drilling. The high-pressure water injected from the backward-facing nozzles also recrushed the collapsed cinder created during punching and increased the flowback flow, helping to avoid borehole blockage by the cinder.

**2.2.4. High-Pressure Drill Pipe.** The design of existing high-pressure drill pipe was improved to include a ring joint on the tip outside of one end of the drill pipe. At the other end of the pipe a circular groove was created inside the pipe that corresponded to the ring joint at the other end. A ring rubber gasket was placed in the bottom of groove to intensify the sealing of the pipe joints. Compared with normal drill pipe, the improved double-layer connected drill pipe had greater joint strength, better sealing effect, and higher security. The structure of the high-pressure drill pipe is shown in Figure 5.

### 3. Analysis of Test Result

#### 3.1. The First Stage Test

**3.1.1. Tests Result.** The first stage adopts punching sequence from coal seam floor to coal seam roof, and the test site is

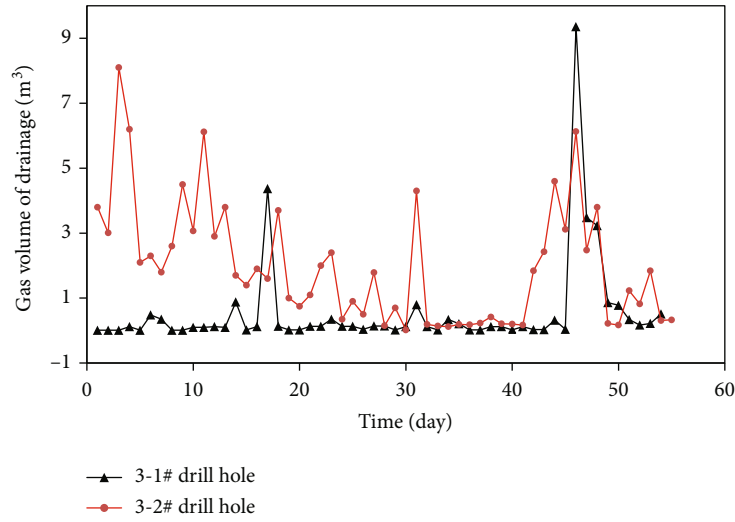


FIGURE 8: Gas extraction in the borehole group 3#.

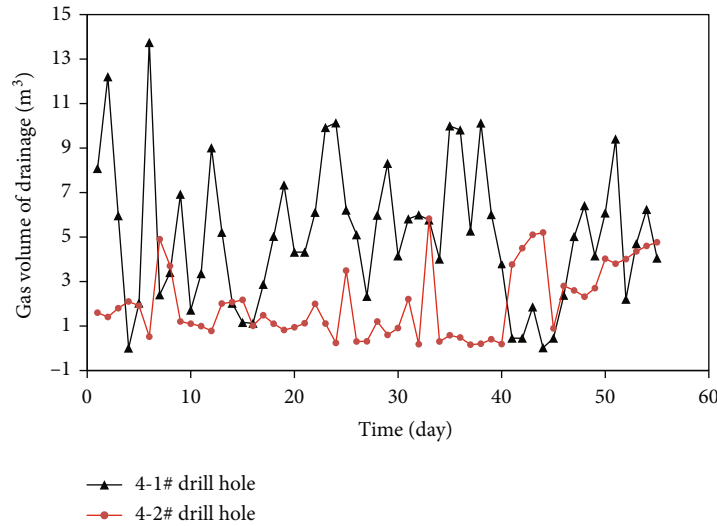


FIGURE 9: Gas extraction in the borehole group 4#.

regarded as the first punching test area. Serious borehole blockage occurred in most boreholes during punching. The cinders that are created by the punching process are mainly distributed in the size range 10~20 mm. However, some cinders have the shape of large flakes with a length of approximately 70 mm.

In the experiments, borehole blockage was most serious in the boreholes 3-1# and 5-1#, in which drill pipe dropping occurred. During punching, the gas concentration at the orifice is always higher than that in other regions of lane the roadway. The spray orifice can result in the gas concentration at the orifice being close to the alarm limit. The more severe is the phenomenon of spraying and blockage in the borehole, the lower is the coal output. The punching data for the first punching area are listed in Table 1.

**3.1.2. Gas Extraction Data.** The boreholes 3-1# and 5-1# exhibited the most serious spraying and borehole blockage

and had relatively small coal output. The average gas extraction volume from 3-1# and 5-1# boreholes was  $0.63 \text{ m}^3$  and  $4.2 \text{ m}^3$ , respectively, while from the corresponding reference boreholes, it was  $2.01 \text{ m}^3$  and  $8.03 \text{ m}^3$ , respectively. These volumes were both lower than the gas extraction of the corresponding reference boreholes. The other average gas extraction volumes which from the punched boreholes 1-1#, 2-1#, 4-1#, and 6-1# were, respectively,  $1.4 \text{ m}^3$ ,  $3.5 \text{ m}^3$ ,  $5.18 \text{ m}^3$ , and  $5.5 \text{ m}^3$ , while the average gas flow from the reference boreholes 1-2#, 2-2#, 4-2#, and 6-2# was, respectively,  $1.3 \text{ m}^3$ ,  $1.23 \text{ m}^3$ ,  $2.1 \text{ m}^3$ , and  $2.7 \text{ m}^3$ .

**3.1.3. Effect Analysis.** As shown in Figures 6–11, for the boreholes 3-1# and 5-1# in which drill pipe dropping occurred, the gas extraction was 0.3 and 0.52 times, respectively, that of reference boreholes. For the boreholes 1-1#, 2-1#, 4-1#, and 6-1# in which only the phenomenon of spraying and borehole blockage occurred, the extraction gas volumes were

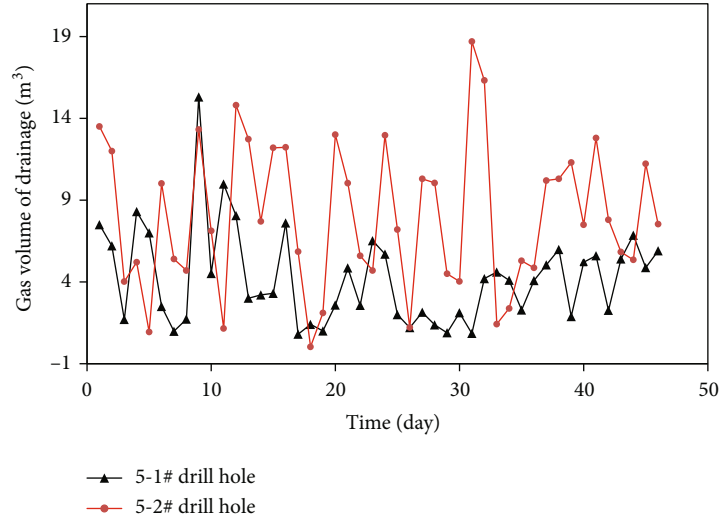


FIGURE 10: Gas extraction in the borehole group 5#.

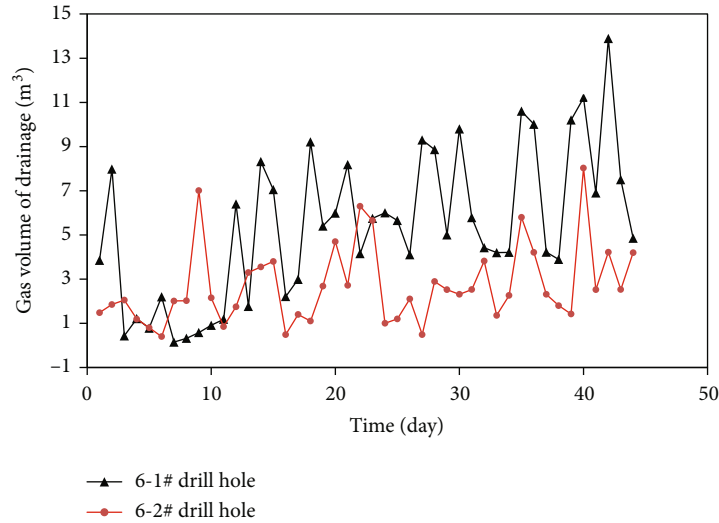


FIGURE 11: Gas extraction in the borehole group 6#.

1.08, 2.85, 2.46, and 2.03 times those of the corresponding reference boreholes. These results indicated that the more serious was blockage of the borehole, the poorer was the gas extraction. The more coal that comes out of the borehole at essentially the same level of plugging, the better the gas extraction affects the borehole.

### 3.2. The Second Stage Test

**3.2.1. Tests Result.** The second stage test adopted the punching sequence from coal seam roof to coal seam floor, and the test site was regarded as the second hydraulic punching area. In view of the serious blockage phenomenon in the previous punching test, the high-pressure triangular drill pipe was used to crush the broken coal slag by secondary extrusion, so as to avoid the occurrence of large-scale coal slag and no drill pipe loss occurred during punching.

TABLE 2: Test parameters in the first punching area.

Borehole number	Quality of discharge (t)	Jet pressure (MPa)	Jet flow (L/min)
7-1#	3.3	15	208
8-1#	3.7	16	215
9-1#	3.2	16	215

However, as the hydraulic punching sequence proceeded from the coal seam roof to coal seam floor step by step, serious spraying and borehole blockage occurred during each punching operation, leading to the gas concentration at the aperture of the punched borehole exceeding the alarm value and forcing a power cut-off accident.

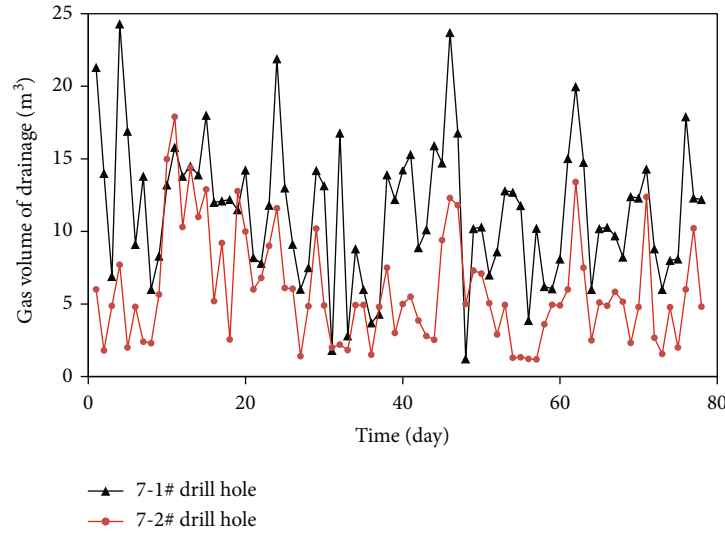


FIGURE 12: Gas extraction in the borehole group 7#.

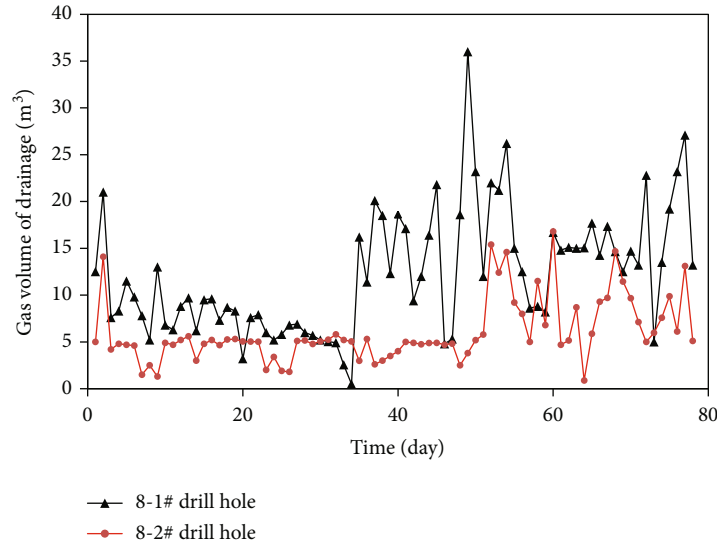


FIGURE 13: Gas extraction in the borehole group 8#.

Because there existed a major safety problem for the punching manner, thrice punching was only carried out in the area. The parameters of the second punching test are listed in Table 2.

**3.2.2. Extraction Data.** As shown in Figures 12–14, the coal output from the punched boreholes 7-1#, 8-1#, and 9-1# was lower and amounted to only 3.3 t, 3.7 t, and 3.2 t, respectively. The average gas volume of extraction from 7-1#, 8-1#, and 9-1# boreholes was  $11.3 \text{ m}^3$ ,  $12.4 \text{ m}^3$ , and  $14.3 \text{ m}^3$ , respectively, while the average gas extraction of the contrasting boreholes 7-2#, 8-2#, and 9-2# was  $5.9 \text{ m}^3$ ,  $5.98 \text{ m}^3$ , and  $4.7 \text{ m}^3$ , respectively. The gas extraction volumes of the punched drill holes were 1.9, 2.07, and 3.04 times, respectively, those of the corresponding reference holes.

### 3.3. The Third Stage Test

**3.3.1. Tests Result.** In the third stage, on the basis of the previous two punching tests, the self-developed crushing coal slag flow-increasing device was adopted, and the forward nozzle of the crushing coal slag flow-increasing device and the high-pressure nozzle on the high-pressure nozzle were used to constitute the first-stage high-pressure crushing of coal mass and buried coal block. By the backward-facing nozzles of the flow-increasing and cinder-breaking device, the secondary crushing was carried out for the broken cinder. Meanwhile, the water yield of deslagging increased during punching, ensuring sufficient backflow from punching to transport and remove the coal cinder. Through the high-pressure triangular drill pipe, the tertiary crushing in the whole borehole section was carried out for the flowback coal cinder.



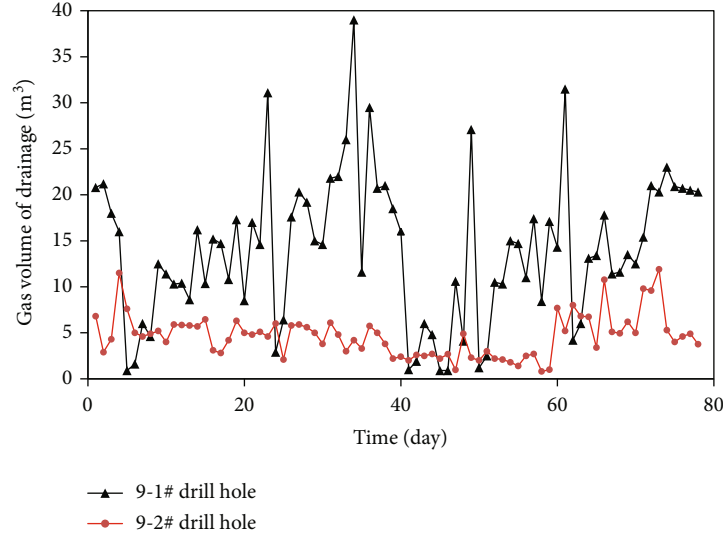


FIGURE 14: Gas extraction in the borehole group 9#.

In the third punching area, the hydraulic punching system experienced no blocking or sticking in the borehole. The cinder particle size was generally less than 5 mm, and the coal cinder flowed back smoothly. A gas leak occurred in the punched borehole 15-1#. In the later period of the test, the gas extraction from the group of boreholes was not measured. The relevant punching parameters for the third test are shown in Table 3.

**3.3.2. Gas Extraction Data.** As shown in Figures 15–19, the average gas extraction of the punched boreholes 10-1#, 11-1#, 12-1#, 13-1#, and 14-1# was  $51.3 \text{ m}^3$ ,  $55.8 \text{ m}^3$ ,  $69.5 \text{ m}^3$ ,  $60.4 \text{ m}^3$ , and  $48 \text{ m}^3$ , respectively, while the average gas extraction of the corresponding reference boreholes 10-2#, 11-2#, 12-2#, 13-2#, and 14-2# was  $13.3 \text{ m}^3$ ,  $7.6 \text{ m}^3$ ,  $12.1 \text{ m}^3$ ,  $9.2 \text{ m}^3$ , and  $9.7 \text{ m}^3$ , respectively. The gas extraction of the punched boreholes was 3.9–7.3 times that of the reference boreholes.

#### 4. Test of Impact of Punching Technique on Influence Radius

The test to examine the impact of punching technique on influence radius was located in the fourth extraction unit in the eastern floor roadway 1308-2#. The effect of punching manner on the influencing radius of the borehole was analyzed in this test, under the conditions of identical coal output. Three groups of punched test boreholes were drilled. In each group, six boreholes were used for observation and one borehole was used for punching. The coal output of each borehole for punching was 6 t, and an average of 0.75 t of coal was removed per meter. As the same borehole layout was used in each group of observation boreholes, thus, only the arrangement of borehole group 1# is given, as shown in Figure 20. In view of the many drill holes, only the boreholes for observation in which the influence radius was successfully investigated are reported.

TABLE 3: Test parameters in the first punching area.

Borehole number	Quality of discharge (t)	Jet pressure (MPa)	Jet flow (L/min)
10-1#	5	15	301
11-1#	4.6	16	311
12-1#	4.7	16	311
13-1#	6	17	320
14-1#	5.5	15	301
15-1#	6.5	17	320

In the first group of boreholes for observation, the first type of hydraulic punching procedure was used. (as described in Section 3.1). During punching, the drill pipe dropping occurred and had great effects on the punch efficiency. In the second group of boreholes for observation, the second punching procedure was used. (as described in Section 3.2). The spraying and borehole blockage were serious during punching. The third punching technique was used in the third group of boreholes for observation. (as described in Section 3.3). The backwater and deslagging were smooth, and there was no spraying or borehole blockage during punching.

As shown in Figure 21(a), the distance between borehole 1-4# to the punched borehole 1# was 4 m. After punching, the gas extraction volume from borehole 1-4# increased by 3.8 times than that before punching. As shown in Figure 21(b), the drill hole for observation 2-1# was 3 m away from the punched drill hole. The gas extraction volume after punching  $0.98 \text{ m}^3/\text{d}$  significantly decreased by 10.3 times in comparison with that before punching  $10.1 \text{ m}^3/\text{d}$ . The reasons for this result were that the high-pressure water used in the punching technique impacted and broke the coal seam structure and extruded and permeated the coal and rock mass. However, borehole blockage resulted in the



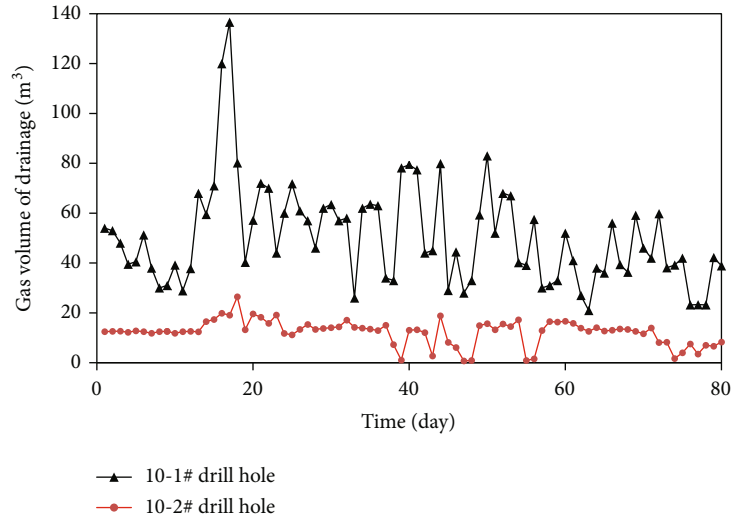


FIGURE 15: Gas extraction in the borehole group 10#.

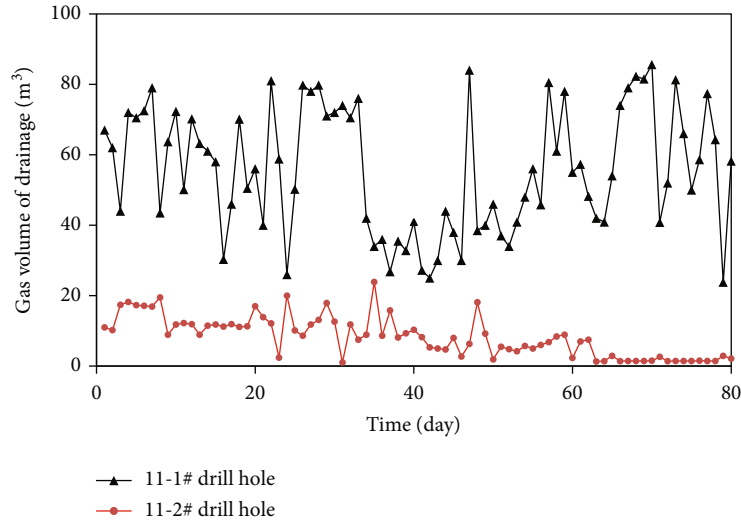


FIGURE 16: Gas extraction in the borehole group 11#.

accumulation of large quantities of high-pressure water that influenced the gas extraction efficiency of the borehole. Thus, after the hydraulic punching, the gas extraction changed significantly increased or decreased, indicating that the borehole 2-1# was located within the radius of influence of the punched borehole.

As shown in Figure 21(c), the distance between observation borehole 3-3# and the borehole for punching was 5 m. The average gas extraction volume from this borehole was  $8.4 \text{ m}^3/\text{d}$  before hydraulic punching and  $53.8 \text{ m}^3/\text{d}$  after hydraulic punching, an increase of 6.4 times. This result, combined with those from boreholes 1-4# and 2-1# illustrates that, under the conditions of identical coal output during punching, the more serious is borehole blockage, the smaller is the radius of influence for the punching borehole. In the absence of borehole blockage, a punched borehole has

a larger radius of influence. Different punching techniques cause large differences in the radius of influence for the punching borehole.

## 5. Discussion

**5.1. Relationship between Punching Sequence and Borehole Blockage.** Comparing the test results of different punching sequences, the top-to-bottom punching sequence has a higher frequency of blockage and is more likely to result in dropped boreholes and blowouts. The reasons for this phenomenon are as follows: on the one hand, when punching from the top of the coal seam to the bottom of the coal seam, the length of the slag removal section is longer [23]. On the other hand, the coal body around the borehole wall is deformed with new fissures during the drilling process, and

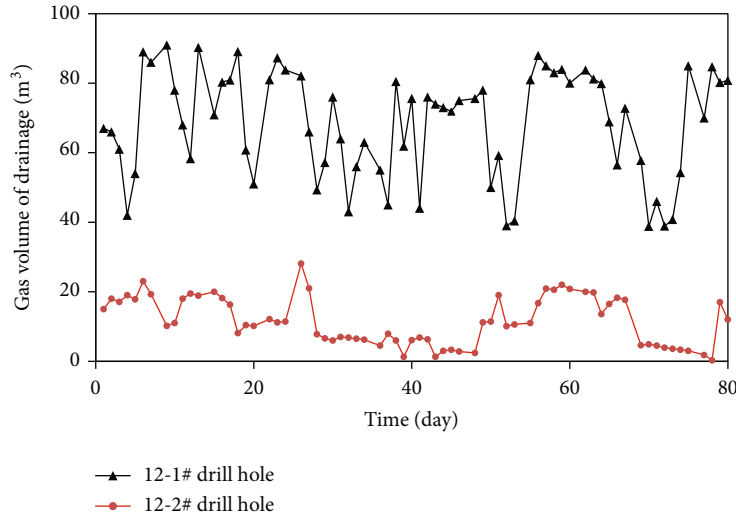


FIGURE 17: Gas extraction in the borehole group 12#.

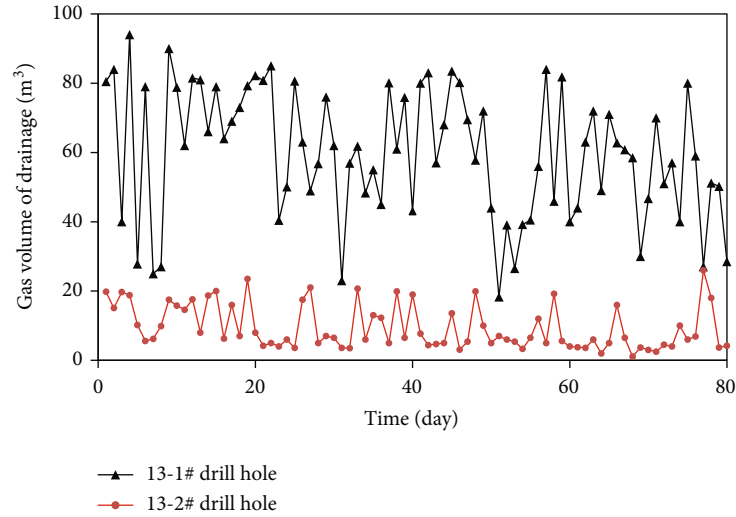


FIGURE 18: Gas extraction in the borehole group 13#.

its strength is reduced under the softening effect of the returned slag water, resulting in the failure of the broken slag to be discharged from the borehole in time and the occurrence of blockage. The second reason is when punching from the bottom to the top, only the rock section of the borehole is responsible for slag removal. The length of the slag discharge section is shorter, and the stability of the rock section borehole is stronger, so the cinder water can be effectively discharged from the borehole, and the blockage phenomenon is not easy to occur.

**5.2. The Relationship between Borehole Blockage and Impact Radius.** Under the impact damage of high-pressure water, a large amount of coal body is broken and spalled, at the same time, the pore fissures in the coal body are opened, which accelerates the creep displacement of the coal body around the borehole and increases the influence radius. After block-

age occurs, the high-pressure water accumulates in the borehole, and the high-pressure water jet gradually evolves into a submerged jet that significantly reduces the efficiency of punching and breaking coal while limiting the disturbance range of the high-pressure water jet [24, 25], which is not conducive to the expansion of coal body pore fissures. Tests on the influence of the punching method on the radius of influence illustrate that the extent of the radius of influence of a punching borehole depends not only on the amount of coal coming out of the punching borehole but also on whether the borehole is plugged. Therefore, optimizing the punching process and eliminating the occurrence of blockage will help to improve the radius of influence of the punched borehole.

**5.3. The Relationship between Borehole Blockage and the Effectiveness of Gas Extraction.** The occurrence of borehole

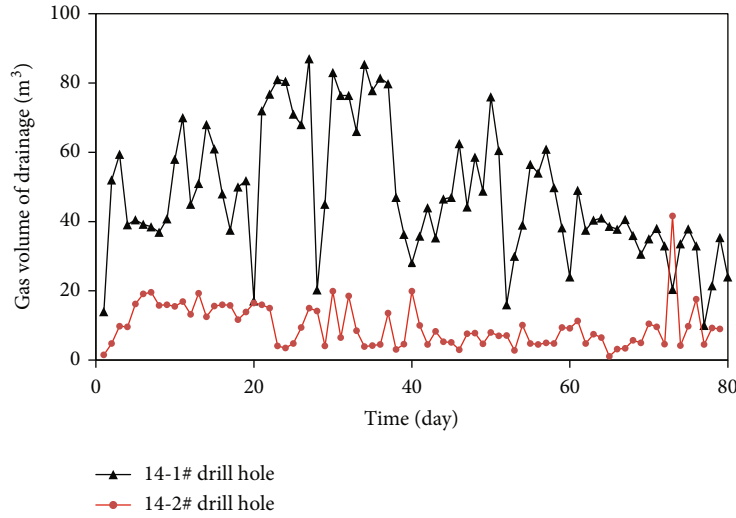


FIGURE 19: Gas extraction in the borehole group 14#.

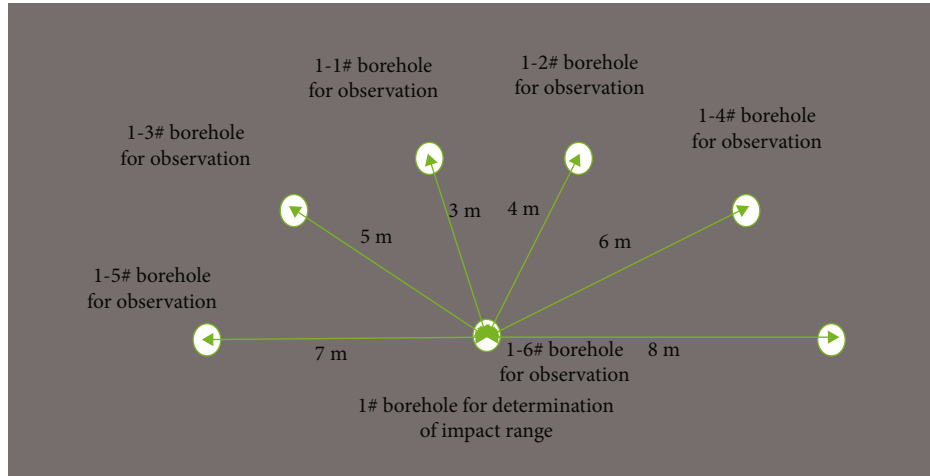


FIGURE 20: Borehole layout of hole group 1# in the influence radius test.

blockage leads to a large collection of high-pressure water in the borehole, and a large amount of water enters the pores and fissures of the coal body that inhibits the desorption of coal seam gas as well as blocks the gas seepage channels, reducing the efficiency of gas extraction in hydraulic perforated boreholes. Boreholes with smooth water drainage have little or no interference with the normal gas extraction of the borehole due to the low infiltration of high-pressure water into the coal seam [26]. Sampling and analysis of coal around the borehole with and without borehole blockage found that the water content of the coal around the plugged and unplugged boreholes was significantly higher than the water content of the coal around the unplugged boreholes with the highest water content in the coal around the boreholes where the drill pipe drop occurred. The results of the water content measurements are shown in Table 4.

*5.4. Relationship between Borehole Blockage and High-Pressure Water Flow.* The causes of borehole blockage can

be divided into two parts. Firstly, punching water volume is too little compared to punching crushed cinder, and the ability of returning water to discharge cinder is too weak [27], resulting in a large amount of cinder collecting in the borehole and the phenomenon of borehole blockage. Secondly, a large amount of cinder water collects in the borehole, and the mechanical properties are weakened under the effect of hydration and “argillization” [28], which adheres to the drill pipe and nozzle around the borehole intensifying the occurrence of blockage.

A three-stage hydraulic punching device for breaking coal and increasing flow is developed for borehole blockage mechanism. The flow-increasing device for crushing coal slag can effectively avoid the ring-plug effect by crushing large size coal slag. By increasing the number of outlet nozzles of high-pressure water and improving the water pressure of pumping station, the outlet water pressure of high-pressure nozzle meets the coal-breaking pressure and increases the punching flow, which ensures that the

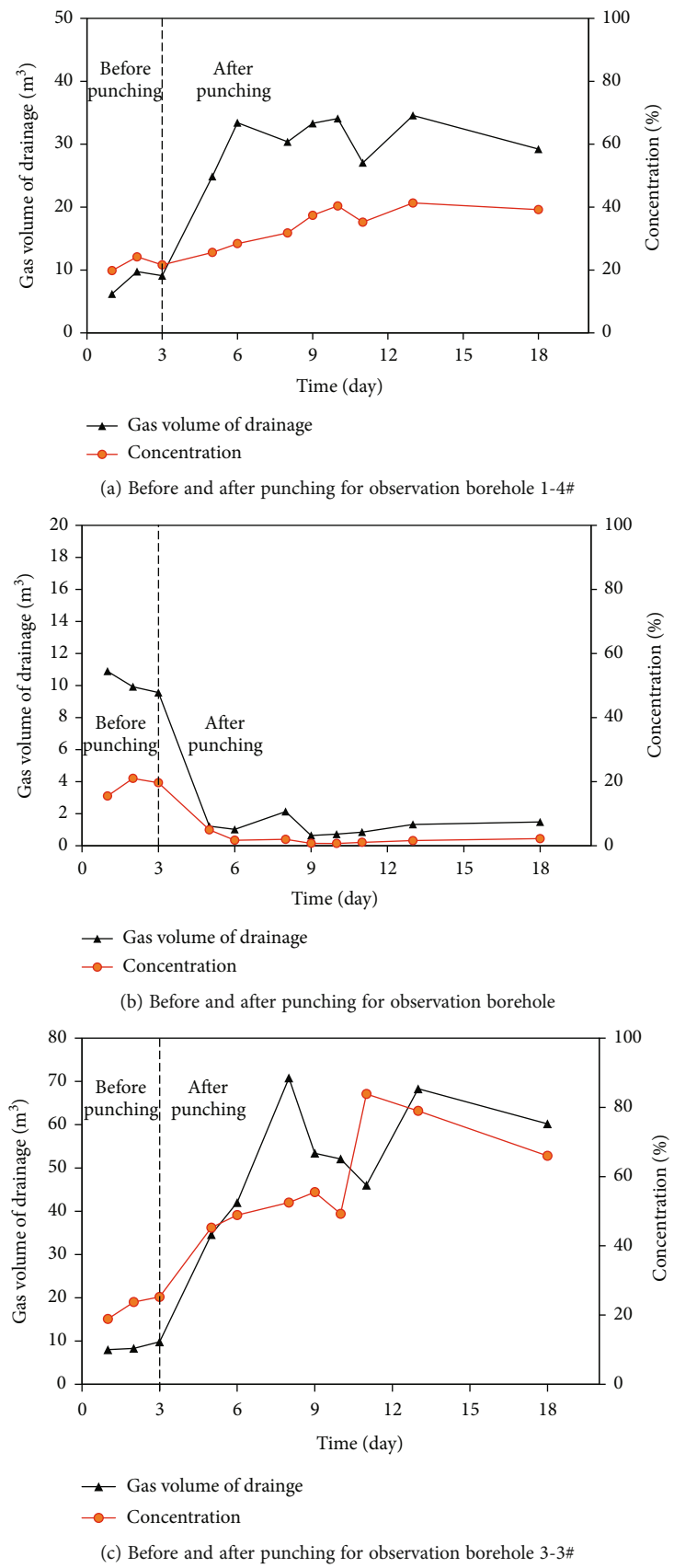


FIGURE 21: Gas extraction volume and concentration from boreholes used for observation in tests investigating the radius of influence of a punched borehole.

TABLE 4: Moisture contents of coal as a function of the condition of boreholes.

Condition of borehole	Moisture content of surrounding coal (%)
Without blockage	1
	1.4
With blockage	5.2
	5.7
With blockage and causing drill pipe dropping	8.4
	9.2

punching return water can effectively discharge coal slag. The high-pressure triangular drill pipe is used to break the returned coal slag twice along the way, so as to avoid the occurrence of large coal slag that is not completely broken and ensure the complete return of punching coal slag.

## 6. Conclusions

As a highly effective gas management technology, each element of the technology deserves in-depth theoretical study to advance the development of hydraulic punching technology. However, an in-depth study of only one of these factors does not meet the need to optimize the overall process of hydraulic punching. The main conclusions can be drawn as follows:

- (1) Borehole blockage can result in high-pressure water being injecting into and permeating the coal seam, occupying gas seepage channels and decreasing permeability. Reducing borehole blockage is conducive to improving the gas extraction efficiency of punched boreholes
- (2) Compared with the effects encountered when punching from the coal seam floor to the coal seam roof, spraying and borehole blockage are encountered more frequently when punching from the coal seam roof to the coal seam floor. Thus, it is more efficient to conduct borehole punching from the bottom to the top of a coal seam than from the top to the bottom
- (3) For any given coal output, different punching techniques cause large differences in the radius of influence of boreholes. Thus, it is crucial to optimize the punching technique to increase radius of influence of punched boreholes and drilling efficiency
- (4) The three-level flow-increasing hydraulic punching system examined in this study effectively prevents borehole blockage and improves the gas extraction efficiency of punched boreholes

## Data Availability

No data are used to support this study.

## Conflicts of Interest

The authors declare that they have no conflicts of interest.

## References

- [1] L. Zhao, H. Dong, J. J. Tang, and J. J. Cai, "Cold energy utilization of liquefied natural gas for capturing carbon dioxide in the flue gas from the magnesite processing industry," *Energy*, vol. 105, pp. 45–56, 2016.
- [2] Y. N. Zheng, Q. Z. Li, C. C. Yuan et al., "Influence of temperature on adsorption selectivity: coal-based activated carbon for CH<sub>4</sub> enrichment from coal mine methane," *Powder Technology*, vol. 347, pp. 42–49, 2019.
- [3] H. Wen, Z. Li, J. Deng et al., "Influence on coal pore structure during liquid CO<sub>2</sub>-ECBM process for CO<sub>2</sub> utilization," *Journal of CO<sub>2</sub> Utilization*, vol. 21, pp. 543–552, 2017.
- [4] H. Wen, X. J. Cheng, J. Chen et al., "Micro-pilot test for optimized pre-extraction boreholes and enhanced coalbed methane recovery by injection of liquid carbon dioxide in the Sangshuping coal mine," *Process Safety and Environmental Protection*, vol. 136, pp. 39–48, 2020.
- [5] W. Wang, H. Li, Y. W. Liu, M. J. Liu, H. F. Wang, and W. Li, "Addressing the gas emission problem of the world's largest coal producer and consumer: lessons from the Sihe Coalfield, China," *Energy Reports*, vol. 6, pp. 3264–3277, 2020.
- [6] A. Y. Zhu, Q. F. Wang, D. Q. Liu, and Y. H. Zhao, "Analysis of the characteristics of CH<sub>4</sub> emissions in China's coal mining industry and research on emission reduction measures," *International Journal of Environmental Research and Public Health*, vol. 19, no. 12, p. 7408, 2022.
- [7] X. L. Yang, G. G. Wen, H. T. Sun et al., "Environmentally friendly techniques for high gas content thick coal seam stimulation—multi-discharge CO<sub>2</sub> fracturing system," *Journal of Natural Gas Science and Engineering*, vol. 61, pp. 71–82, 2019.
- [8] J. Z. Liu, H. T. Sun, Y. Lei, and J. Cao, "Current situation and development trend of coalbed methane development and utilization technology in coal mine area," *Journal of China Coal Society*, vol. 45, no. 1, pp. 258–267, 2020.
- [9] G. Bai, J. Su, Z. G. Zhang et al., "Effect of CO<sub>2</sub> injection on CH<sub>4</sub> desorption rate in poor permeability coal seams: an experimental study," *Energy*, vol. 238, article 121674, 2022.
- [10] Z. L. Wang, S. X. Sang, X. Z. Zhou, and X. D. Liu, "Numerical study on CO<sub>2</sub> sequestration in low-permeability coal reservoirs to enhance CH<sub>4</sub> recovery: gas driving water and staged inhibition on CH<sub>4</sub> output," *Journal of Petroleum Science and Engineering*, vol. 214, article 110478, 2022.
- [11] L. Qin, C. Zhai, J. Z. Xu, S. M. Liu, C. Zhong, and G. Q. Yu, "Evolution of the pore structure in coal subjected to freeze–thaw using liquid nitrogen to enhance coalbed methane extraction," *Journal of Petroleum Science and Engineering*, vol. 175, pp. 129–139, 2019.
- [12] H. Li, S. Shi, B. Lin et al., "Effects of microwave-assisted pyrolysis on the microstructure of bituminous coals," *Energy*, vol. 187, article 115986, 2019.
- [13] H. D. Wang, Z. H. Cheng, Q. L. Zou et al., "Elimination of coal and gas outburst risk of an outburst-prone coal seam using controllable liquid CO<sub>2</sub> phase transition fracturing," *Fuel*, vol. 284, article 119091, 2021.
- [14] Y. Lei, J. J. Liu, S. N. Zhang, W. Zhang, and H. D. Wang, "Contrast test of different permeability improvement technologies

- for gas-rich low-permeability coal seams,” *Journal of Natural Gas Science and Engineering*, vol. 33, pp. 1282–1290, 2016.
- [15] Q. T. Hu, L. Liu, Q. G. Li et al., “Experimental investigation on crack competitive extension during hydraulic fracturing in coal measures strata,” *Fuel*, vol. 265, article 117003, 2020.
  - [16] Y. Zhao, B. Q. Lin, T. Liu, Q. Z. Li, and J. Kong, “Gas flow field evolution around hydraulic slotted borehole in anisotropic coal,” *Journal of Natural Gas Science and Engineering*, vol. 58, pp. 189–200, 2018.
  - [17] Y. K. Ma, X. Y. Mao, K. Yang, J. Liu, and A. H. Zhao, “Improvement on gas drainage of soft gassy coal seam with underground hydraulic flushing and fracturing: a case study in Huainan,” *Arabian Journal of Geosciences*, vol. 13, no. 4, 2020.
  - [18] R. Zhang, Y. P. Cheng, L. Yuan, H. X. Zhou, L. Wang, and W. Zhao, “Enhancement of gas drainage efficiency in a special thick coal seam through hydraulic flushing,” *International Journal of Rock Mechanics and Mining Sciences*, vol. 124, article 104085, 2019.
  - [19] Y. P. Fan, L. Y. Shu, Z. G. Huo, J. W. Hao, and Y. Li, “Numerical simulation of sectional hydraulic reaming for methane extraction from coal seams,” *Journal of Natural Gas Science and Engineering*, vol. 95, article 104180, 2021.
  - [20] H. Wang, E. Y. Wang, Z. H. Li et al., “Study on safety pressure of water jet breaking coal based on the characteristic analysis of electromagnetic radiation signal,” *Process Safety and Environmental Protection*, vol. 144, pp. 284–296, 2020.
  - [21] Z. L. Ge, S. R. Cao, Y. Y. Lu, and F. F. Gao, “Fracture mechanism and damage characteristics of coal subjected to a water jet under different triaxial stress conditions,” *Journal of Petroleum Science and Engineering*, vol. 208, article 109157, 2022.
  - [22] X. Zhao, Y. Li, G. Lv et al., “Specification for the Identification of Coal Mine Gas Grades GB40880-2021,” State Mine Safety Supervision Bureau, People's Republic of China, 2021.
  - [23] Y. L. Wang, Z. J. Yu, and Z. F. Wang, “A mechanical model of gas drainage borehole clogging under confining pressure and its application,” *Energies*, vol. 11, no. 10, p. 2817, 2018.
  - [24] Y. Q. Zhang, X. Y. Wu, X. Hu et al., “Visualization and investigation of the erosion process for natural gas hydrate using water jet through experiments and simulation,” *Energy Reports*, vol. 8, pp. 202–216, 2022.
  - [25] X. F. Yang, “The influence of confining pressure on the flow field structure of submerged water jet,” in *Proceedings of the 5th International Conference on Civil Engineering and Transportation 2015*, vol. 30, pp. 1400–1404, Atlantis Press, 2016.
  - [26] M. Hao, C. M. Wei, and Z. Qiao, “Effect of internal moisture on CH<sub>4</sub> adsorption and diffusion of coal: a molecular simulation study,” *Chemical Physics Letters*, vol. 783, article 139086, 2021.
  - [27] D. Stipić, L. Budinski, and J. Fabian, “Sediment transport and morphological changes in shallow flows modelled with the lattice Boltzmann method,” *Journal of Hydrology*, vol. 606, article 127472, 2022.
  - [28] D. Li, D. S. Wu, F. G. Xu, J. H. Lai, and L. Shao, “Literature overview of Chinese research in the field of better coal utilization,” *Journal of Cleaner Production*, vol. 185, pp. 959–980, 2018.